

Initial-state dependence of phase behaviors in a dense active system

Lu Chen(陈璐), Bokai Zhang(张博凯), and Z. C. Tu(涂展春)

Citation: Chin. Phys. B, 2023, 32 (**8**): 086401. DOI: 10.1088/1674-1056/acca09
Journal homepage: http://cpb.iphy.ac.cn; http://iopscience.iop.org/cpb

What follows is a list of articles you may be interested in

Phase-field study of spinodal decomposition under effect of grain boundary

Ying-Yuan Deng(邓英远), Can Guo(郭灿), Jin-Cheng Wang(王锦程), Qian Liu(刘倩), Yu-Ping Zhao(赵玉平), and Qing Yang(杨卿)

Chin. Phys. B, 2021, 30 (**8**): 088101. DOI: 10.1088/1674-1056/abea9b

Modeling of microporosity formation and hydrogen concentration evolution during solidification of an Al-Si alloy

Qingyu Zhang(张庆宇), Dongke Sun(孙东科), Shunhu Zhang(章顺虎), Hui Wang(王辉), Mingfang Zhu(朱鸣芳)

Chin. Phys. B, 2020, 29 (**7**): 078104. DOI: 10.1088/1674-1056/ab8abb

Material microstructures analyzed by using gray level Co-occurrence matrices

Yansu Hu(胡延苏), Zhijun Wang(王志军), Xiaoguang Fan(樊晓光), Junjie Li(李俊杰), Ang Gao(高昂)

Chin. Phys. B, 2017, 26 (**9**): 098104. DOI: 10.1088/1674-1056/26/9/098104

The effect of two-dimensional shear flow on the stability of a crystal interface in the supercooled melt

Cao Bin (曹斌), Lin Xin (林鑫), Wang Meng (王猛), Huang Wei-Dong (黄卫东)

Chin. Phys. B, 2012, 21 (**8**): 086401. DOI: 10.1088/1674-1056/21/8/086401

Linear stability analysis on a spherical particle growing from a binary melt under the far-field flow

Cao Bin(曹斌), Lin Xin(林鑫), Wang Meng(王猛), and Huang Wei-Dong(黄卫东)

Chin. Phys. B, 2012, 21 (**5**): 056401. DOI: 10.1088/1674-1056/21/5/056401

Initial-state dependence of phase behaviors in a dense active system

Lu Chen(陈璐)[1,2,†], Bokai Zhang(张博凯)[3], and Z. C. Tu(涂展春)[1]

[1] *Department of Physics, Beijing Normal University, Beijing* 100875, *China*
[2] *Complex Systems Division, Beijing Computational Science Research Center, Beijing* 100193, *China*
[3] *School of Physical Science and Technology, Southwest University, Chongqing* 400715, *China*

(Received 29 December 2022; revised manuscript received 12 February 2023; accepted manuscript online 4 April 2023)

There are rich emergent phase behaviors in non-equilibrium active systems. Flocking and clustering are two representative dynamic phases. The relationship between both the phases is still unclear. Herein, we numerically investigate the evolution of flocking and clustering in a system consisting of self-propelled particles with active reorientation. We consider the interplay between flocking and clustering phases with different initial configurations, and observe a domain in steady state order parameter phase diagrams sensitive to the choice of initial configurations. Specifically, by tuning the initial degree of polar ordering, either a more ordered flocking or a disordered clustering state can be observed in the steady state. These results enlighten us to manipulate emergent behaviors and collective motions of an active system, and are qualitatively different from the emergence of a new bi-stable regime observed in aligned active particles due to an explicit attraction [*New J. Phys.* **14** 073033 (2012)].

Keywords: initial state, flocking, clustering, active systems

PACS: 64.70.dg, 81.30.–t, 05.60.Cd, 07.05.Tp **DOI:** 10.1088/1674-1056/acca09

1. Introduction

Active systems have attracted much attention from researchers in interdisciplinary fields.[1–4] The emergence of collective motion appearing in such systems inspires us to consider the dynamics in the evolution process of active systems. However, unlike an equilibrium system determined by the principle of minimum free energy, these systems are far from equilibrium. So far, there is still no widely acknowledged theory to describe the steady-state phase behaviors since nonequilibrium evolution is usually dependent on system's dynamic paths, which is an interesting property commonly observed in many living and engineered systems.[5–9]

In the past few decades, extensive work has been performed towards initial states in network, natural and social systems.[10–15] A series of intriguing behaviors emerge along with different dynamic paths. In addition, experiments usually show more complex structures or patterns probably due to the processing routes or transition pathways (history).[16–22] In particular, one of the main manifestation of history dependence is initial-state dependence.[23] In recent years, many studies have shown that initial velocity distributions can influence formation of coherent structures,[24] nonequilibrium criticality of magnetic systems,[25] and alignment of block copolymer microdomains.[26] In the work reported in Ref. [27], Großmann *et al.* considered a model of active Brownian particles with velocity alignment. They found that the system can relax into different stable states starting from different initial conditions (passive noise, active speed noise, and active angular fluctuations), which make us consider whether this result also exists in other active models.

In this work, we focus on the impact of initial states on the emergent behaviors in an active system of self-propelled particles based on a model we developed previously.[28] In this model, an active reorientation rule is incorporated for particles at collisions, to mimic the collision avoidance behavior commonly adopted in cell colonies,[29,30] animal herds,[31,32] swarming robots,[33] and traffic flows.[34] The coupling between self-propulsion and active reorientation produces richer dynamics compared with previous models merely involving translation or rotation. As a result, these particles may collectively aggregate to dynamic clusters or self-organize into aligned flocking. In our current work, we study history-dependent properties in this active system, and explore how the initial states influence dynamic path and eventually the steady state of the system. Specifically, with different initial states we observe distinctive steady states as illustrated by the phase diagram of flocking and clustering. The phase boundary is considered to come from the competition between active reorientation and noise. It is sensitive to initial distribution of particle position and orientation. Interestingly, the system could evolve into one of two nonequilibrium stable states by manipulating initial states. All these findings offer a new way to control collective behaviors by adjusting dynamic paths.

2. Model system and simulation method

In previous studies, many emergent behaviors can be well characterized by imposing explicit local alignment interactions,[35] an inelastic collision rule,[36] or a separation

[†]Corresponding author. E-mail: lu_chen@mail.bnu.edu.cn
© 2023 Chinese Physical Society and IOP Publishing Ltd

of time scales between orientation and propulsion.[37,38] However, none of these models explicitly include collision avoidance in their rules of interaction, a strategy commonly adopted by motile animals in a herd.[39,40] In this study, we consider an active collision avoidance model developed in our previous work.[28] The model consists of self-propelled disks with a diameter d in a plane. Here, $\boldsymbol{r}_i$ and $\boldsymbol{n}_i \equiv (\cos\theta_i, \sin\theta_i)$ represent the position and self-propulsion direction of disk i ($i = 1, \ldots, N$).

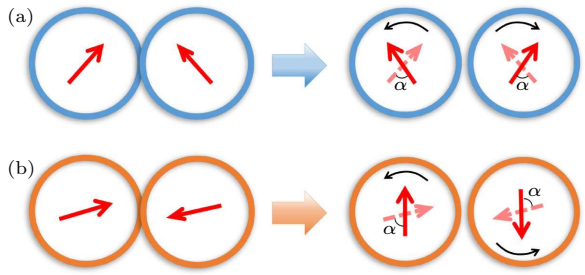


Fig. 1. Schematic diagrams of collision avoidance by active reorientations.

The dynamics of the i-th disk is determined by the following equations:

$$\partial_t \boldsymbol{r}_i = v_0 \boldsymbol{n}_i \prod_{j\neq i}^{N} [1 - \varepsilon(r_{ij} - d)] + \sum_{j=1, j\neq i}^{N} k(d - r_{ij})\varepsilon(d - r_{ij}) \frac{\boldsymbol{r}_i - \boldsymbol{r}_j}{r_{ij}}, \quad (1)$$

$$\partial_t \theta_i = \sum_{j=1, j\neq i}^{N} \alpha\delta(t)\varepsilon(d - r_{ij}) \left(\frac{\boldsymbol{r_j} - \boldsymbol{r_i}}{r_{ij}} \times \boldsymbol{n}_i \right) \cdot \hat{\boldsymbol{z}} + \eta_i(t). \quad (2)$$

The first equation describes translation of disk i. The first term $v_0\boldsymbol{n}_i$ represents the self-propulsion velocity along $\boldsymbol{n}_i$. The second term represents the contribution of collision when two disks come close to each other. Here, d is diameter of disk; $r_{ij} = |\boldsymbol{r}_j - \boldsymbol{r}_i|$ is the distance between the centers of disk i and disk j; $\varepsilon(x)$ is the Heaviside function. If $r_{ij} < d$, then $\varepsilon = 1$, otherwise $\varepsilon = 0$. Parameter k represents the ratio of strength of two-body interaction between disks to coefficient of friction. The second equation describes rotation of disk i. When disk i is free, it rotates due to Gaussian white noise η_i which satisfies $\langle \eta_i(t) \rangle = 0$ and $\langle \eta_i(t)\eta_j(t') \rangle = \frac{\sigma^2}{2}\delta_{ij}\delta(t - t')$, with $\alpha\delta(t)$ being the angular velocity, which is generated as an result of active reorientation acting on the colliding disks. We $\hat{\boldsymbol{z}}$ as a normal vector of the plane pointing the reader, and choose $\alpha > 0$ in order to mitigate the collision between two disks in collision. This idea of effective collision avoidance is shown in Fig. 1. We numerically solve Eqs. (1) and (2) using periodic boundary conditions with square box of length L. The relevance of crowding is controlled by the packing fraction

$$\phi = \frac{N\pi(d/2)^2}{L^2}. \quad (3)$$

In our simulation, we use particle diameter and simulation time step as the units for length and time, respectively, and fix self-propulsion velocity $v_0 = 0.1$ and coefficient $k = 1.0$. We check the finite size effect by studying systems of different sizes up to 16000 particles. Little difference is observed for systems with 1000 or more particles. In this paper, we fix packing fraction $\phi = 0.3$ with particle number $N = 1000$ to explore the kinetic properties of the system.

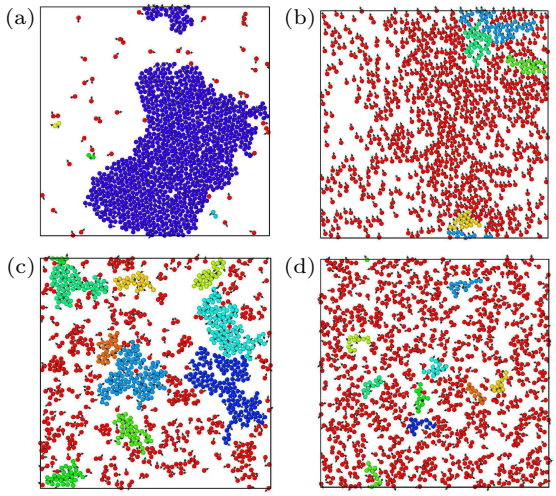


Fig. 2. Representative steady states: (a) clustering (steady state with $\alpha = 0.01$, $\sigma = 0.04$); (b) flocking (steady state with $\alpha = 0.01$, $\sigma = 0.01$); (c) partly disordered phase (steady state with $\alpha = 0.02$, $\sigma = 0.06$); (d) totally disordered phase (steady state with $\alpha = 0.01$, $\sigma = 0.10$). The arrows indicate the direction of orientation [$\boldsymbol{n}_i = (\cos\theta_i, \sin\theta_i)$]. Colors (except red) represent different clusters.

With v_0 fixed, the dynamics of the system is controlled by two parameters: the noise strength σ and active reorientation angle α. We have tested that the influence of self-propulsion speed on our system is mainly associated with the formation of cluster or living crystal states, such as the emergence of hexatic and solid order in Ref. [41], which has little effect on dynamics. However, a certain amount of noise is necessary so as to induce a non-equilibrium phase separation.[42] Therefore, in this paper, we focus on the effects of noise and active reorientation on the dynamic behaviors of the system. For each given set of σ and α, we first place particles at random locations with random orientations, as initial states to simulate the evolution of the system. Figures 2(a)–2(d) present some possible collective behaviors that arise from different evolutionary processes. As orientations of particles are evolved by actively reorienting themselves and rotational diffusion with $\alpha = 0.01$, $\sigma = 0.04$, we find the formation of clusters as shown in Fig. 2(a). Figure 2(b) shows a flocking state in which the orientations of all particles are approximately aligned while the position distribution is uniform. Figures 2(c) and 2(d) present two kinds of disordered phases. One includes small clusters even though the orientations of particles are isotropic. The other is totally disordered since the orientation and position of particles are in uniform distribution.

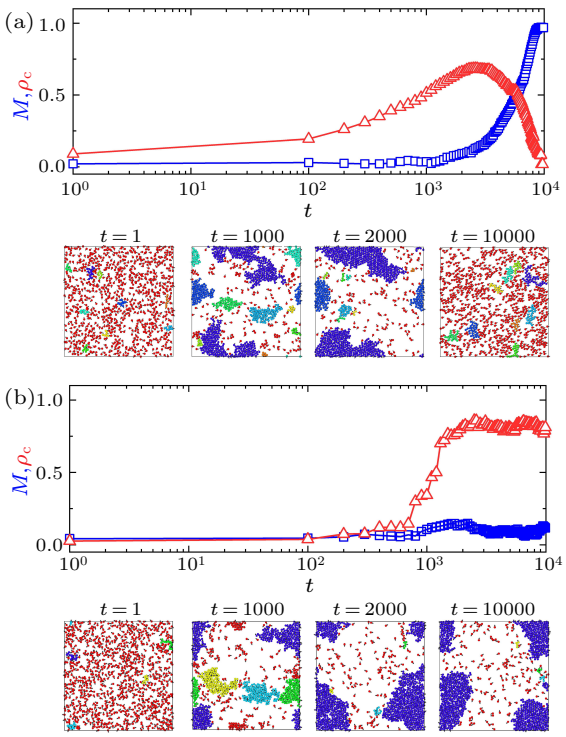


Fig. 3. Temporal evolution of order parameters and configurations. The system eventually evolves to (a) flocking state under $\alpha = 0.01$, $\sigma = 0.02$, and (b) clustering state under $\alpha = 0.01$, $\sigma = 0.04$.

2.1. Order parameters

We introduce two order parameters to characterize the steady states of the system mentioned above. Flocking appearing in our system is described by an orientational order parameter

$$M = \sqrt{\langle \cos\theta \rangle_N^2 + \langle \sin\theta \rangle_N^2}, \tag{4}$$

where the average $\langle\ \rangle_N$ is taken over all N particles. $M \approx 1$ indicates the perfect flocking phase and $M \approx 0$ the disordered phase. To quantitatively identify the phase of the system that separates into dense clustered state and dilute gas-like state, we measure the local area density of each particle as

$$a_l = \frac{A}{A_v}. \tag{5}$$

Here a_l is the area of each disk normalized by the area A_v of the Voronoi cell for each disk.[43,44] By numerical simulation, we find that when a_l is larger than a certain threshold, the disk is located in the dense cluster. In this work, we set the threshold as 0.7. We introduce order parameter ρ_c to describe clustering. ρ_c is the fraction of particles with $a_l > 0.7$. These two order parameters can give a good description of the degree of flocking and clustering. In Figs. 2(a)–2(d), we show four configurations as examples: clustering without flocking ($M \approx 0, \rho_c \approx 0.92$), flocking without clustering ($M \approx 1, \rho_c \approx 0$), partly clustering partly flocking ($M \approx 0.7, \rho_c \approx 0.26$), disordered ($M \approx 0, \rho_c \approx 0$). In order to explore the dynamics of flocking and clustering, we analyze the time series of M and ρ_c. In our previous study,[28] we showed system dynamics for two parameter choices: $\alpha = 0.01$, $\sigma = 0.01$, and $\alpha = 0.01$, $\sigma = 0.1$, where the results demonstrated that flocking and MIPS are mutually exclusive. In the present study, system dynamics at other parameter choices is presented, which supports such a conclusion. For example, Fig. 3(a) shows the time series under parameter $\alpha = 0.01$ and $\sigma = 0.02$. We use 100 ensembles to average to get M and ρ_c as functions of time. M grows slowly first, then sharply increases and eventually reaches flocking state with M close to 1. Thereat, ρ_c grows slowly at the beginning, then it reaches a transient plateau. Concurrent with the sharp increase of M, the transient plateau of ρ_c collapses. The snapshots of the configurations are shown below Fig. 3(a). When the system starts from a disordered state, small clusters appear in the system, and phase separation is triggered. Then the condensation nuclei come together and aggregate into a large cluster. Also, the non-equilibrium clustering appearing in the system was observed in other active models.[45–47] Next, as particles collide with each other, scattering with active reorientation competes with the self-diffusion process. As a result, the cluster gradually disintegrates and disperses. The final state of the system is highly flocking, similar to the flocking state in the Vicsek model.[48] In contrast, as shown in Fig. 3(b), under the parameters $\alpha = 0.01$ and $\sigma = 0.04$, ρ_c increases on a time scale similar to that in Fig. 3(a) and finally saturates at around 0.8, whereas M remains low throughout the simulation. The evolution of configuration is relatively simple. Particles interact with each other and gradually form stable clusters. There is no orientational order in the steady state.

2.2. Steady state phase diagrams

The order parameters would fluctuate little for a long enough time. In our model, the system reaches a steady state after a few thousands of time steps. Thus, in order to characterize steady states, we measure the order parameters at 10000 time steps under different sets of $\{\alpha, \sigma\}$. Here we initiate our simulations by placing particles with random locations and random orientations.

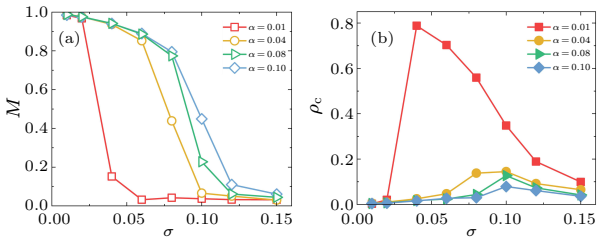


Fig. 4. The dependence of (a) M and (b) ρ_c on σ with $\alpha = 0.01$, 0.04, 0.08, 0.10.

In Fig. 4, we present the dependence of M and ρ_c on σ with $\alpha = 0.01$, 0.04, 0.08, 0.10. As shown in Fig. 4(a), when α is fixed, the system finally presents order or disorder state,

which depends on the intensity of noise. With the increasing α, the parameter σ at critical phase transition point also increases. As shown in Fig. 4(b), similar behavior also manifests in the aggregation of clusters. In particular, the value of σ at critical phase transition point for flocking and clustering is the same. The overall phase behavior can be understood by considering the competition between the absorption rate of particles into clusters and escape rate of particles from clusters. When a particle collides with a cluster, it has a probability either entering or escaping from the cluster due to active reorientation and noise. In the diagram of ρ_c, the regions with a high degree of clustering correspond to the regions where global alignment cannot be formed in the diagram of M. High global flocking and large cluster cannot coexist with each other.

3. Effects of initial states on clustering and flocking

In equilibrium systems, the phase transition is usually independent of the initial state. However, this argument may not hold for non-equilibrium systems. Therefore, in this section, we explore the influence of initial states, such as effects of the distribution of particle initial orientations on temporal evolution and steady state behaviors of order parameter M and ρ_c.

3.1. Effects of initial states on phase diagrams

The M_0 denotes the value of the orientational order parameter of the initial state. We change the initial states of the system from the homogeneous state to the highly flocking state. Specifically, in our previous study[28] we investigated the steady state phase diagrams of M and ρ_c with $M_0 = 0$. In the present study, we change the initial states of the system from the homogeneous state with $M_0 = 0$ to other states with $M_0 = 0.2$, 0.6, and 1.

With new initial states, we study the corresponding steady phase diagrams. Figures 5(a)–5(f) represent phase diagrams of M and ρ_c in the steady state under the initial state from low alignment to highly alignment condition. Comparing these phase diagrams of M and ρ_c in Fig. 5, as the initial conditions M_0 change, we can find that the phase diagrams also change. The phase separation line obviously shifts when α is relatively small. The flocking domain in Fig. 5(a) is broader than that in Fig. 5(e). For the phase diagram of ρ_c, on the contrary, the clustering domain in Fig. 5(b) becomes smaller than the domain in Fig. 5(f). Next we quantitatively characterize the difference between these diagrams. Figure 6(a) shows ΔM, which is the difference between orientational order parameters in the steady states under two different initial states ($M_0 = 0, 1$) mentioned above. The differences are concentrated in the dark area. Likewise, we present $\Delta\rho_c$, which is the difference between ρ_c under the same condition in Fig. 6(b). We observe that they are quite similar to each other, almost matching up in the same domain. Then we define correlation C_{cor} as

$$C_{cor} = \frac{\int \Delta\rho_c \Delta M \, d\alpha d\sigma}{\sqrt{\int (\Delta\rho_c)^2 \, d\alpha d\sigma \int (\Delta M)^2 \, d\alpha d\sigma}}. \tag{6}$$

By calculating the correlation between the two phase diagrams, we find that the correlation is about 60.43%, which suggests that correlation among flocking (clustering) states under different initial conditions is strong.

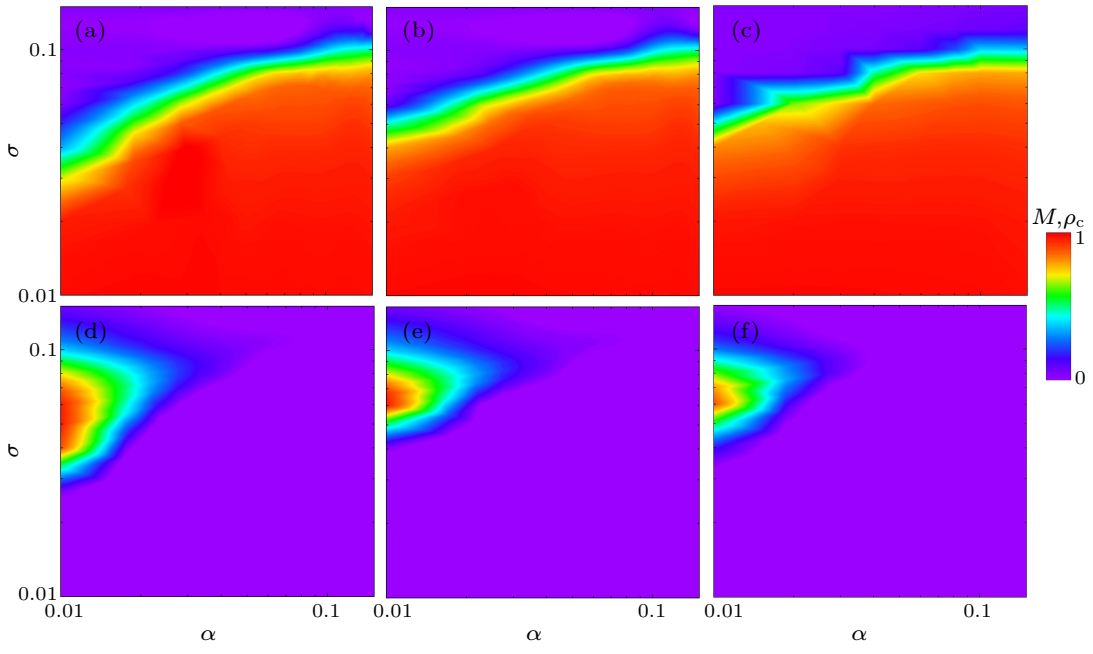


Fig. 5. Phase diagrams of steady states starting from low alignment condition ($M_0 \sim 0.2$), middle alignment condition ($M_0 \sim 0.6$), and highly alignment condition ($M_0 \sim 1.0$). [(a), (c), (e)] Phase diagrams of M under the initial conditions $M_0 \sim 0.2$, $M_0 \sim 0.6$, and $M_0 \sim 1.0$, respectively. [(b), (d), (f)] Phase diagrams of ρ_c under the initial conditions $M_0 \sim 0.2$, $M_0 \sim 0.6$, and $M_0 \sim 1.0$, respectively.

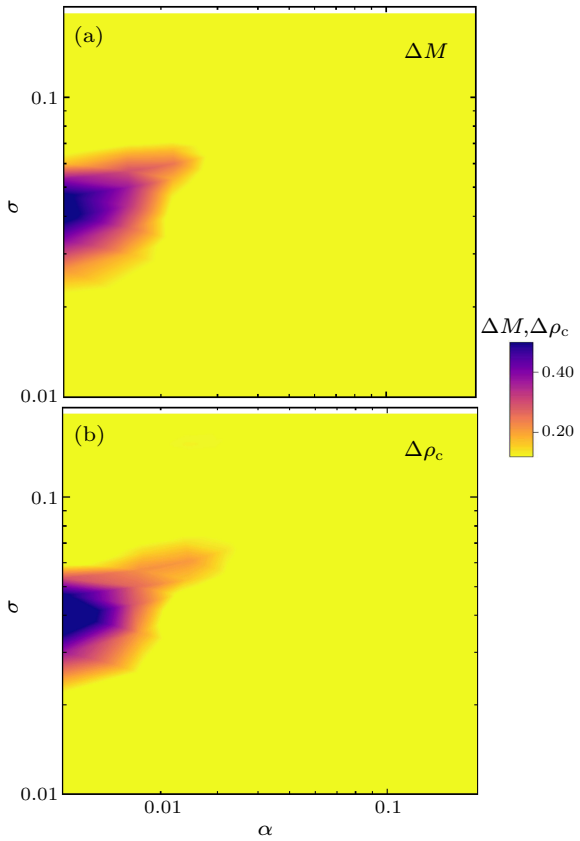


Fig. 6. (a) Difference of M between the flocking diagram ($M_0 = 0$) and the phase diagram shown in Fig. 5(e) ($M_0 = 1$). (b) Difference of ρ_c between the clustering diagram ($M_0 = 0$) and the phase diagram shown in Fig. 5(f) ($M_0 = 1$).

3.2. Influence of initial states on the evolutionary process and steady states

In order to study how initial states affect the evolution of a system, we choose two sets of parameters in different regions. One set of parameters is $\alpha = 0.01$ and $\sigma = 0.01$, which belongs to the region that the steady state is not sensitive to the initial state. The other set is $\alpha = 0.01$ and $\sigma = 0.04$, which belongs to the region that the steady state is sensitive to the initial state. Figures 7(a) and 7(b) show the evolution of M with time under different initial states. Figures 7(c) and 7(d) show the ρ_c likewise. Figures 7(a) and 7(c) reveal that the growth of M is synchronized with the growth of ρ_c under different M_0. Meanwhile, the ability of clustering decreases with the increase of M_0. Therefrom, we understand that it is initial states that affect the evolution of the system, reflecting on the change of cluster formation and local alignment. In the above case, the initial state affects the evolution of the system, but does not affect steady states at all. Furthermore, we explore another case of $\alpha = 0.01$ and $\sigma = 0.04$, which is in the domain sensitive to initial states. From Figs. 7(b) and 7(d), we observe that the system finally stabilizes at different amplitudes with different initial states when the system reaches steady states. We realize that different initial states of the system lead to distinct non-equilibrium steady states in the certain critical domain.

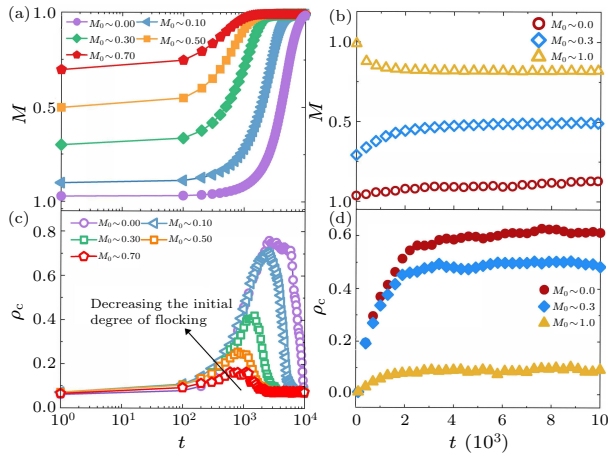


Fig. 7. Time evolution of M and ρ_c from different initial states with parameters $\alpha = 0.01$, $\sigma = 0.01$ (left) and $\alpha = 0.01$, $\sigma = 0.04$ (right).

3.3. Distribution of order parameters in the steady state

For those systems with steady state $M \approx 0.5$ obtained by averaging 100 independent runs, we investigate the distribution of M and ρ_c.

As for the steady states in the domain which is insensitive to initial states, Figs. 8(a) and 8(b) reveal that the distributions of M and ρ_c in the steady states is totally located at around 1 and 0, respectively. However, in the domain which is sensitive to initial states, according to the distributions shown in Figs. 8(c) and 8(d), we can see that it is possible to move from the bistable regime into the only disordered regime or ordered regime by decreasing or increasing M_0. We would like to emphasize that such behaviors only appear in the specific domain of the phase diagrams. So far, we bring out the existence of a metastability regime which is affected by initial states. However, we still need a understanding of phase-ordering kinetics because the absence of a well-defined notion of temperature and free energy of these systems far from equilibrium makes it difficult to get insights from a theoretical point of view.

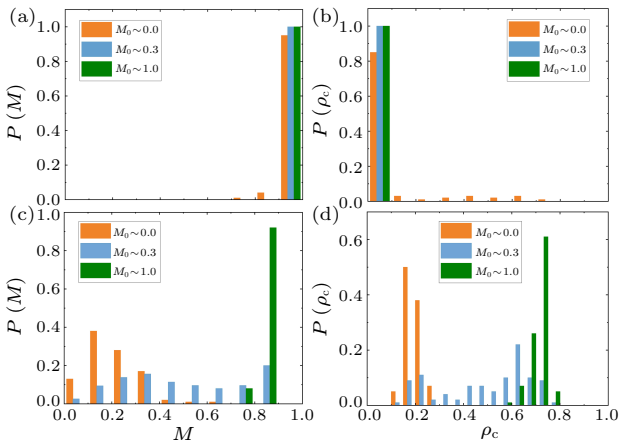


Fig. 8. Distribution of order parameters in steady states. [(a), (b)] The distributions of M and ρ_c with parameters $\alpha = 0.01$ and $\sigma = 0.01$. [(c), (d)] The distributions of M and ρ_c with parameters $\alpha = 0.01$ and $\sigma = 0.04$.

4. Conclusion

In summary, we have investigated the influence of initial states on the evolution process and steady state of the active system based on a model with active reorientation. The system displays rich phase behaviors including global flocking, clustering and disordered phases. We observe an interesting interplay between flocking and clustering. We notice that the boundaries of flocking phase and clustering phase rely on the choice of initial states. Although clustering is like a high nucleation barrier that prevents the system from escaping from metastable states,[49] the increasing order degree of initial states would suppress clustering during the process of self-organization evolution. In the meantime, we find that there is an instable region in our model, in which the system will relax to different steady states due to different initial conditions. This is consistent with the results of active Brownian particles using the velocity-alignment theory proposed by Großmann *et al.*[27] However, the difference of our model from Großmann *et al.* is that our model has no effective alignment interaction between individual particles. In addition, under the competition between external noise and active angular fluctuations, our system can bypass some states that should be experienced under different initial conditions, that is, the dynamic path, it evolves into different stable states. Since dynamic path can influence evolution behaviors of a self-organizing system, active matter or active robots may be controlled to allow the system to grow towards an expected state from the perspective of regulation. This finding has a wide range of applications in improving designs of collective migration and navigation strategies.

Acknowledgments

We thank X. L. Xu for helpful suggestion. We also acknowledge computational support from the Beijing Computational Science Research Center. The research was supported by the National Natural Science Foundation of China (Grant Nos. U2230402, 11975050, 11735005, and 11904320).

References

[1] Li H, Shi X Q, Huang M, Chen X and Zhang H P 2019 *Proc. Natl. Acad. Sci. USA* **116** 777
[2] Shi X Q, Fausti G, Chaté H, Nardini C and Solon A 2020 *Phys. Rev. Lett.* **125** 168001
[3] Li H, Yang X and Zhang H P 2020 *Chin. Phys. B* **29** 060502
[4] Li Y, Li L, Marchesoni F, Debnath D and Ghosh P K 2020 *Phys. Rev. Res.* **2** 013250
[5] Mayergoyz I D 2006 *The Science of Hysteresis: Physical Modeling, Micromagnetics, and Magnetization Dynamics* (Oxford: Gulf Professional Publishing) p. 33
[6] Huang M and Sethna J P 1991 *Phys. Rev. B* **43** 3245
[7] Erpelding M, Sinha S, Tallakstad K T, Hansen A, Flekkøy E G and Måløy K J 2013 *Phys. Rev. E* **88** 053004
[8] Banerjee S, Patil N and Ramakrishnan S, Grover A K, Bhattacharya S, Mishra P K, Ravikumar G, Chandrasekhar Rao T V, Sahni V C, Higgins M J, Tomy C V, Balakrishnan G and Paul D M 1999 *Phys. Rev. B* **59** 6043
[9] Zhao N N, Saavedra S and Liu Y Y 2021 *Phys. Rev. E* **103** 052403
[10] Yu C T, Cui K P, Guo H L, Ye Y N, Li X Y, and Gong J P 2021 *Macromolecules* **54** 9927
[11] Munck B D 2022 *J. Interdisciplin. History* **52** 565
[12] Qian W, Papadopoulos L, Lu Z, Kroma-Wiley K A, Pasqualetti F and Bassett D S 2022 *Phys. Rev. E* **105** 024304
[13] Grötsch R K, Wanzke C, Speckbacher M, Angl A, Rieger B and Boekhoven J 2019 *J. Am. Chem. Soc.* **141** 9872
[14] Tsay J J and Arora J S 1990 *Comput. Method. Appl. Mech. Eng.* **81** 183
[15] Medeiros E S, Medrano-T R, Caldas I L, Tél T and Feudel U 2019 *Phys. Rev. E* **100** 052201
[16] González-López K, Mahajan S, Zheng Y, Ciamarra M P and Lerner E 2021 *Phys. Rev. E* **103** 022606
[17] Eule S and Metzger J J 2016 *New J. Phys.* **18** 3033006
[18] Ballauff M, Brader J M, Egelhaaf S U, Fuchs M, Horbach J, Koumakis N, Kr'uger M, Laurati M, Mutch K J, Petekidis G, Siebenbürger M, Voigtmann T and Zausch J 2013 *Phys. Rev. Lett.* **110** 215701
[19] Papanikolaou S, Tzimas M, Reid A and Langer S A 2019 *Phys. Rev. E* **99** 053003
[20] Ranjkesh A, AmbroDiI A, Cordoyiannis G, Kutnjak Z and Kralj S 2013 *Adv. Condens. Matter Phys.* 2013 505219
[21] Henderson W, Andrei E, Higgins M and Bhattacharya S 1996 *Phys. Rev. Lett.* **77** 2077
[22] Kwon S and Sung B J 2020 *Phys. Rev. E* **102** 022501
[23] Maitra N, Burke K and Woodward C 2002 *Phys. Rev. Lett.* **89** 023002
[24] Karimov A R and Schamel H 2001 *Phys. Plasmas* **8** 1180
[25] Prudnikov V N, Prudnikov P and Lyakh A S 2020 *Phys. Solid State* **62** 821
[26] Schmidt K, Böker A, Zettl H, Schubert F, Hänsel H, Fischer F, Weiss T M, Abetz V, Zvelindovsky A V, Sevink G J A and Krausch G 2005 *Langmuir* **21** 11974
[27] Großmann R, Schimansky-Geier L and Romanczuk P 2012 *New J. Phys.* **14** 073033
[28] Chen L, Welch K J, Leishangthem P, Ghosh D, Zhang B K, Sun T P, Klukas J, Tu Z C, Cheng X and Xu X L 2023 arXiv:2302.10525 [cond-mat.soft]
[29] Nagy M, Akos Z, Biro D and Vicsek T 2010 *Nature* **464** 890
[30] Kamdar S, Shin S, Leishangthem P, Francis L, Xu X L and Cheng X 2022 *Nature* **603** 819
[31] Bialek W, Cavagna A, Giardina I, Mora T, Silvestri E, Viale M and Walczak A M 2012 *Proc. Natl. Acad. Sci. USA* **109** 4786
[32] Frewen T A, Couzin I D, Kolpas A, Moehlis J, Coifman R and Kevrekidis I G 2011 *Lecture Notes in Computational Science and Engineering* **75** 299
[33] Keya J, Akter M, Kabir A, Rashid M and Kakugo A 2022 *Methods Mol. Biol.* **2430** 219
[34] Zhou W Q, Guo H X and Yao L H 2023 *Sustainability* **15** 1832
[35] Vicsek T, Czirók A, Ben-Jacob E, Cohen I and Shochet O 1995 *Phys. Rev. Lett.* **75** 1226
[36] Grossman D, Aranson I S and Ben-Jacob E 2008 *New J. Phys.* **10** 023036
[37] Lam K D, Schindler M and Dauchot O 2015 *New J. Phys.* **17** 113056
[38] Lam K D and Schindler M and Dauchot O 2015 *J. Stat. Mech.: Theory Exp.* **2015** P10017
[39] Moussaïd M, Helbing D and Theraulaz G 2011 *Proc. Natl. Acad. Sci. USA* **108** 6884
[40] Chan R W and Gabbiani F 2013*J. Exp. Biol.* **216** 641
[41] Digregorio P, Levis D, Suma A, Cugliandolo L F, Gonnella G and Pagonabarraga I 2018 *Phys. Rev. Lett.* **121** 098003
[42] Levis D and Berthier L 2014 *Phys. Rev. E* **89** 062301
[43] Martin-Roca J, Martinez R, Alexander L C, Diez A L, Aarts D G, Alarcon F, Ramírez J and Valeriani C 2021 *J. Chem. Phys.* **154** 164901
[44] Stenhammar J, Marenduzzo D, Allen R J and Cates M E 2014 *Soft Matter* **10** 1489
[45] Peruani F, Deutsch A and Bär M 2006 *Phys. Rev. E* **74** 030904
[46] McCandlish Ro, Baskaran A and Hagan M 2012 *Soft Matter* **8** 2527
[47] Chaté H, Ginelli F, Grégoire G, Peruani F and Raynaud F 2018 *Eur. Phys. J. B* **64** 451
[48] Vicsek T, Czirók A, Ben-Jacob E, Cohen I and Shochet O 2006 *Phys. Rev. Lett.* **75**
[49] Levis D, Codina J and Pagonabarraga I 2017*Soft Matter* **13** 8113